J Neurophysiol 122: 1735–1744, 2019.
First published August 28, 2019; doi:10.1152/jn.00338.2019.

RESEARCH ARTICLE | *Neural Circuits*

High-definition tDCS to the right temporoparietal junction modulates slow-wave resting state power and coherence in healthy adults

Peter H. Donaldson, Melissa Kirkovski, Joel S. Yang, Soukayna Bekkali, and Peter G. Enticott
School of Psychology, Deakin University, Geelong, Victoria, Australia

Submitted 4 June 2019; accepted in final form 19 August 2019

Donaldson PH, Kirkovski M, Yang JS, Bekkali S, Enticott PG. High-definition tDCS to the right temporoparietal junction modulates slow-wave resting state power and coherence in healthy adults. *J Neurophysiol* 122: 1735–1744, 2019. First published August 28, 2019; doi:10.1152/jn.00338.2019.—The right temporoparietal junction (rTPJ) is a multisensory integration hub that is increasingly utilized as a target of stimulation studies exploring its rich functional network roles and potential clinical applications. While transcranial direct current stimulation (tDCS) is frequently employed in such studies, there is still relatively little known regarding its local and network neurophysiological effects, particularly at important nonmotor sites such as the rTPJ. The current study applied either anodal, cathodal, or sham high-definition tDCS to the rTPJ of 53 healthy participants and used offline EEG to assess the impacts of stimulation on resting state (eyes open and eyes closed) band power and coherence. Temporoparietal and central region delta power was increased after anodal stimulation (the latter trend only), whereas cathodal stimulation increased frontal region delta and theta power. Increased coherence between right and left temporoparietal regions was also observed after anodal stimulation. All significant effects occurred in the eyes open condition. These findings are discussed with reference to domain general and mechanistic theories of rTPJ function. Low-frequency oscillatory activity may exert long-range inhibitory network influences that enable switching between and integration of endogenous/exogenous processing streams.

NEW & NOTEWORTHY Through the novel use of high-definition transcranial direct current stimulation (tDCS) and EEG, we provide evidence that both anodal and cathodal stimulation of the right temporoparietal junction selectively modulate slow-wave power and coherence in distributed network regions of known relevance to proposed temporoparietal junction functionality. These results also provide direct evidence of the ability of tDCS to modulate oscillatory activity at a long-range network level, which may have explanatory power in terms of both neurophysiological and behavioral effects.

coherence; electroencephalogram; high-definition transcranial direct current stimulation; resting state; temporoparietal junction

INTRODUCTION

Transcranial direct current stimulation (tDCS) is used broadly in neuroscience research due to its proposed neuromodulatory effects. However, the importance of better understanding the local and distributed neurophysiological effects of stimulation, particularly with regard to nonmotor stimulation sites, has been increasingly recognized (Sellaro et al. 2016). There are many reasons that this understanding is important. First, assumptions are made regarding the likely effects and mechanisms of stimulation based on motor cortex research, which may not generalize to nonmotor areas. Second, conclusions or claims are often made regarding the behavioral effects, or clinical relevance, of stimulating a particular region, without considering either distributed stimulation effects or the stimulation montage employed. Finally, it is ultimately through an increased understanding of the underlying mechanisms of the effect of stimulation that the broad potential of technologies such as tDCS may be more fully realized.

The right temporoparietal junction (rTPJ) is a multisensory integration hub implicated in functional networks including attention/salience, memory, social cognition, and default mode networks (Carter and Huettel 2013; Igelström et al. 2015, 2016; Kubit and Jack 2013; Mars et al. 2012a, 2012b). While a number of domain-specific theories mapping onto involvement in these networks are posited, several domain-general theories regarding rTPJ processing/functionality also exist. These include the opposing domains and attentional breaking/reorienting hypotheses (Kubit and Jack 2013), acting as an intero-exteroception "switch" subserving integrative predictive processes (Bzdok et al. 2013), contextual updating of internal models (Geng and Vossel 2013), and the nexus model of Carter and Huettel (2013). The nexus model reasons that the TPJ is involved in multisensory and multinetwork integration processes that facilitate decision-making, performance of complex tasks, and establishment of a social context (Carter and Huettel 2013). While these theories differ in nuance, they have in common the theme of a multinetwork integrative role for the TPJ in higher order processes. Such a role implies a need for strong communicative links, implying in turn a need for a mechanism for both local and distant communication, of which resting state network connectivity is one candidate mechanism. Studies examining rTPJ connectivity tend to advocate a parcellation approach and suggest that rTPJ subregions display varying levels of resting state and functional connectivity. Regions implicated comprise the aforementioned functional networks, particularly left temporoparietal sites and central/prefrontal structures (Bzdok et al. 2013; Carter and Huettel 2013; Igelström et al. 2016; Mars et al. 2012b). The rTPJ is also a site of increasing interest with reference to neuromodulatory studies and potential clinical relevance (Donaldson et al. 2015; Eddy 2016).

Address for reprint requests and other correspondence: P. Donaldson, School of Psychology, Deakin Univ., Locked Bag 20000, Geelong, Victoria 3220, Australia (e-mail: peter.donaldson@deakin.edu.au).

Two ways of evaluating the electrophysiological network effects of rTPJ HD-tDCS are electroencephalographic (EEG) resting state power and coherence. Of relevance here is the principle that synchronous oscillations of neural assemblies at particular frequencies, even in nonproximal brain nodes/regions, may subserve brain network communication and function. Two related theories are the communication through coherence (CTC) hypothesis and the gating by inhibition (GBI) hypothesis. The former (CTC) posits that neuronal communication is essentially facilitated by neuronal temporal synchronization, with increased synchrony associated with increased functional communication/connectivity (Fries 2005, 2015; Womelsdorf et al. 2007). The latter (GBI) essentially proposes that information routing between task-relevant regions is mediated by inhibiting/blocking activity in regions less relevant to the task (or current processing) (Jensen and Mazaheri 2010). Importantly, both theories may contribute to overall processing via low-frequency/high-frequency coupling, whereby higher frequency synchronous oscillations may be more associated with local task-related processing (and the CTC framework) and lower frequency oscillations may be critical to longer range communication coordination (via the GBI framework) (Bonnefond et al. 2017; Florin and Baillet 2015).

Application of transcranial electrical stimulation (including tDCS) can influence neural oscillations and cognitive function, perhaps via direct and indirect influences on pyramidal cells and interneurons involved in glutamatergic and GABAergic transmission and local and distributed excitation/inhibition balances (Buzsáki et al. 2012; Harmony 2013; Krause et al. 2013). This relates to the notion that the increased excitability frequently attributed to anodal tDCS is mediated by the effects of reduced local GABA and/or increased glutamate concentrations, which may have both local and network effects, a notion that has some support in motor cortex work (Stagg et al. 2014).

Annarumma et al. (2018) recently summarized results pertaining to both proximal and distal bandwidth power influences of tDCS, suggesting that anodal stimulation was associated with reduced slower wave power (delta, theta, alpha) but increased beta power, while cathodal stimulation increases slower wave power (delta, theta) and reduces beta and gamma power. Regarding the rTPJ more specifically, Spitoni et al. (2013) applied anodal/cathodal/sham tDCS to the right posterior parietal cortex (rPPC: P2, P4, P6; noncephalic reference electrode), reporting that the only significant modulation was postanodal stimulation increases in EEG parietal alpha power and, to a lesser extent, frontal alpha power. Mangia et al. (2014) applied the same protocol to the rPPC (P4; without a cathodal condition). Consistent with the findings of Spitoni et al. (2013), they reported significant increases in alpha power in parietal and frontal regions after anodal stimulation. Additionally, they observed increased theta power parietocentrally during stimulation and frontally after stimulation and increased beta power in parallel with the aforementioned alpha-power modulation, although largely in contralateral parietal electrode sites. Based on these findings, Hsu et al. (2014) attempted to increase alpha power via rPPC (P4) anodal tDCS in a sample to examine subsequent effects on a visual memory task but found alpha power decreased in the low-performing group and did not change in the high-performing group, which they interpreted through a lens of state-dependent tDCS effects. No studies could be identified examining the effects of TPJ tDCS on EEG coherence.

While these studies provide some evidence of stimulation influences on these important metrics of network dynamics, this short literature review also highlights the dearth of knowledge in this domain, further emphasizing the need for increased understanding in such an important nonmotor site as the rTPJ. These studies also used traditional tDCS, which is a disadvantage in terms of degree of acuity (due to large stimulation areas) when assessing and extrapolating with regard to local and distributed electrophysiological effects and potential impacts on function. This study sought to redress these limitations by using electroencephalography (EEG) to assess the impacts of anodal and cathodal rTPJ high-definition transcranial direct current stimulation (HD-tDCS) on resting state power and coherence with regards to key functional network regions associated with the rTPJ (frontal, central, and left TPJ electrode configurations). The limited number of directly relevant prior findings preclude confident directional hypotheses. However, based on the most directly relevant (PPC) studies discussed above, it was hypothesized that anodal stimulation (compared with cathodal and sham stimulation) would increase resting state power in theta, alpha, and beta bandwidths in the region of stimulation and functionally connected regions. It was also predicted that both active stimulation conditions would be associated with coherence changes in these regions compared with sham stimulation.

MATERIALS AND METHODS

The present paper presents data collected as part of a larger study. The methodology therefore overlaps with that described previously in papers examining different aspects of the data set (Donaldson et al. 2018, 2019).

Participants

The sample comprised 53 right-handed healthy volunteers aged 18–40, with normal or corrected-to-normal vision and no contraindications to standard noninvasive brain stimulation screening protocols (Rossi et al. 2009) or history of mental illness, as determined by the MINI International Neuropsychological Interview Screen (Lecrubier et al. 1997). Participant demographics are outlined in Table 1. There were no significant differences between groups on any factor, with the exception of sex. The female-to-male ratio in sham, cathodal, and anodal conditions was 10:8, 14:4, and 6:11, respectively (Cramer's $V = 0.35$, $P = 0.04$). Post hoc testing indicated that cathodal and anodal conditions differed with regards to sex ($P = 0.03$). Time of day tested was also recorded and assessed, as it has been suggested that circadian factors and the physiology of sleep/wake states may mediate plasticity and responses to stimulation (Li et al. 2015). Time of day tested did not differ between groups.

Design

The study was double-blind and sham controlled with both within-subjects (pre- versus poststimulation) and between-subjects (stimulation condition; sham versus cathodal versus anodal stimulation) factors. Participants took part in one session, in which resting state EEG was recorded before and after 20 min of either sham, cathodal, or anodal HD-tDCS to the rTPJ. Protocols were approved by the Human Research Ethics Committee of Deakin University.

Table 1. *Demographic characteristics as per group*

Variable	Sham (n = 18)	Cathodal (n = 18)	Anodal (n = 17)	ANOVA Statistics	
				F	P
Age, yr	26.5 ± 6.6	24.4 ± 4.4	24.3 ± 5.4	0.90	0.41
Education, yr	17 ± 2.6	17.3 ± 2.6	17.4 ± 3.4	0.10	0.91
Time of day tested	11:34 ± 2.6	11:52 ± 2.6	11:00 ± 2.4	0.20	0.82
EHI	0.88 ± 0.2	0.83 ± 0.2	0.85 ± 0.2	0.24	0.79

Values are means ± SD. EHI, Edinburgh Handedness Inventory.

Questionnaires

Participants completed the Edinburgh Handedness Inventory (Oldfield 1971) to confirm right-handedness before participation. At the end of the session (after stimulation and second EEG recording), participants completed a poststimulation questionnaire.

Procedure

Participants were fitted with an EEG cap (https://www.easycap.de/wordpress/), and the 10–20 system sites for HD-tDCS electrodes were marked (Figs. 1 and 2). The cap was then removed. HD-tDCS electrode sites were cleaned with abrasive paste and alcohol swabs before five electrodes were fixed (20-mm diameter circular rubber, supplied by neuroConn; https://www.neurocaregroup.com) into position with adhesive conductive paste. An impedance check was carried out to ensure impedance was <50 kΩ (neuroConn 2014) before the EEG cap was replaced. HD-tDCS electrode positions were rechecked. Thirteen single silver-silver chloride (Ag-AgCl) sintered ring EEG electrodes were fastened to the cap at the sites displayed in Fig. 1. EEG electrodes were also placed on each mastoid, above and below the left eye, and on the lateral canthus of each eye. The ground electrode was placed centrally on the forehead. Conductive gel was then applied to all EEG electrodes. Impedances were kept below 5 kΩ where possible (with all impedances kept below 10 kΩ). Two experimenters completed this setup process. The second experimenter then left the room before the next stage.

Participants were seated in a darkened room, 60 cm from the computer monitor (https://zowie.benq.com/en/product/monitor.html) at eye level. They sat for 2 min during resting state (eyes open) EEG recording, during which they were instructed to focus on a white fixation cross (15 × 15 mm) in the center of the blackened screen (280 × 515 mm). EEG was then recorded for 2 min while participants were asked to keep their eyes closed.

At this point, the second experimenter returned to the room. The first experimenter then left the room to maintain blinding. An impedance check was again carried out on HD-tDCS electrodes. HD-tDCS was then applied to the rTPJ for 20 min (sham, cathodal, or anodal).

After HD-tDCS the first experimenter left the room again and the second experimenter returned. Participants again sat for 2 min during resting state (eyes open) EEG recording, followed by a further 2 min while participants were asked to keep their eyes closed. Finally, participants completed the poststimulation questionnaire.

HD-tDCS

The montage was chosen according to optimal current intensity and focality, based on Soterix neurotargeting software (https://soterixmedical.com/research/software). The configuration, current at each electrode, and modeling of stimulation intensity (for cathodal stimulation) are displayed in Fig. 2. Stimulation was applied using a neuroConn DC-Stimulator (MC Version; https://www.neurocaregroup.com). Active stimulation (anodal or cathodal) applied a current intensity of 2 mA (split evenly between electrodes) for 20 min, with a 30-s ramp-up and ramp-down at the beginning and end. Sham stimulation was also 20 min, but contained only three short, intermittent bursts of active 2-mA stimulation (totaling 230 s, each burst with a 30-s ramp-up and ramp-

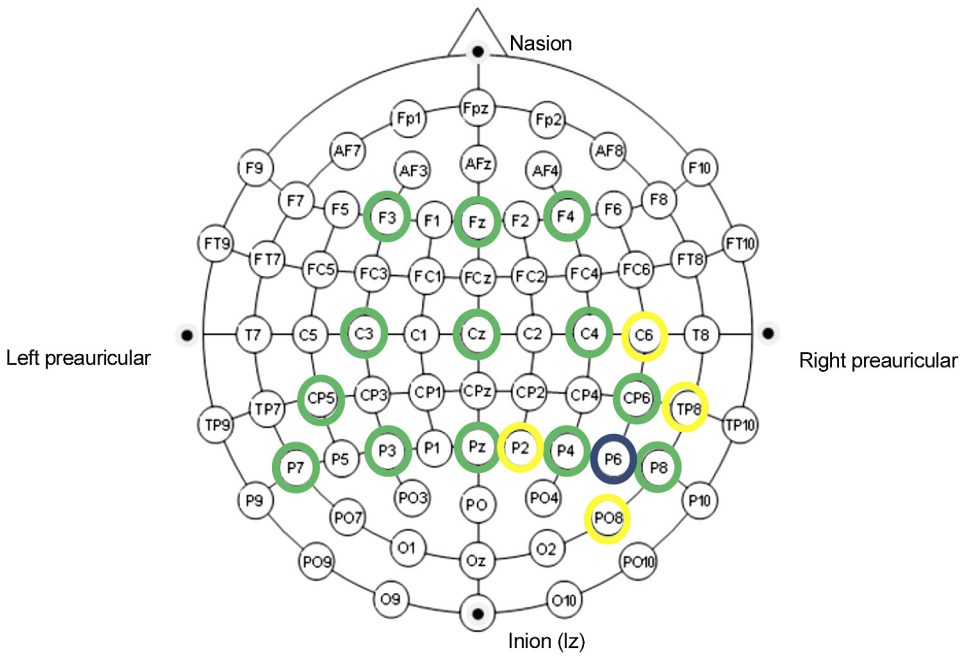

Fig. 1. Diagram of EEG electrode layout (green circles) and high-definition-transcranial direct current stimulation (HD-tDCS) electrode montage (yellow circles: 0.5 mA each, navy blue: circle 2 mA, polarity depending on anodal or cathodal condition). Electrodes were also placed on each mastoid, above and below the left eye, and on the lateral canthus of each eye. The ground electrode was placed centrally on the forehead.

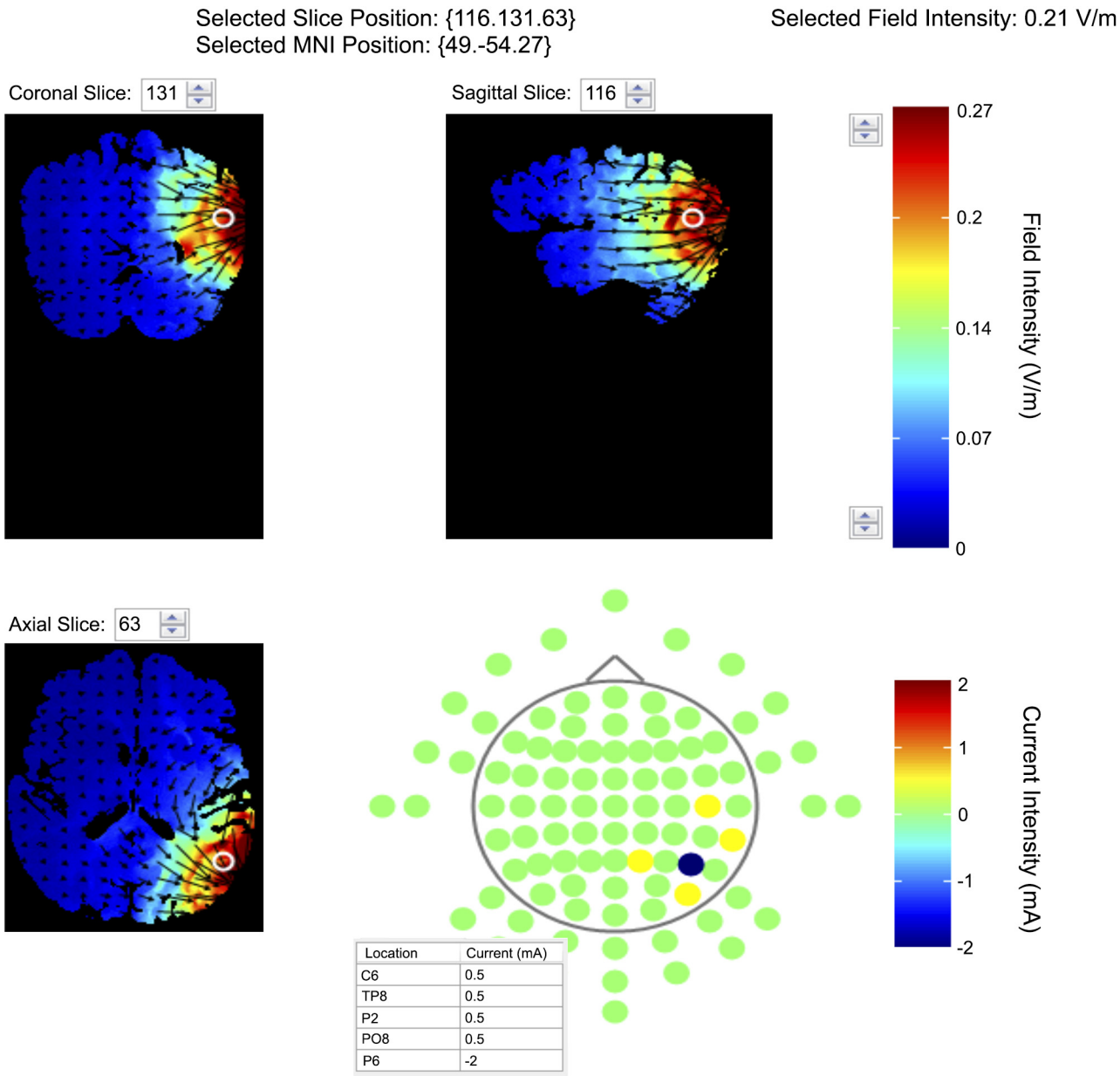

Fig. 2. Montage and Soterix modeling for cathodal stimulation of the right temporoparietal junction (rTPJ). Polarities are reversed for anodal stimulation. For anodal stimulation, the central electrode (P6) was the anode, with the other 4 electrodes (C6, TP8, PO8, and P2) collectively forming the cathode (see also Fig. 1). The reverse polarity arrangement constituted cathodal stimulation. MNI, Montreal Neurological Institute.

down). Participants were seated in a nondarkened room during stimulation, and were not engaged in any activities. EEG was not recorded during stimulation.

EEG Recording and Preprocessing

A 64-channel SynAmpsRT amplifier was used for acquisition (Compumedics Neuroscan, Charlotte, NC; https://compumedicsneuroscan.com/). EEG recordings were in DC at a sampling rate of 1000 Hz.

EEG data were processed and analyzed offline using Curry 7 Neuroimaging Suite (https://compumedicsneuroscan.com/). Data were baseline corrected (constant), rereferenced to the average of the two mastoids and band pass filtered (1–30 Hz). Oculomotor artefacts were identified (vertical, 100 uV; horizontal, 130 uV) and covaried. Bad blocks were also identified (±75 uV, as well as visually) and marked for exclusion from further analysis.

For resting state power analysis, back-to-back 1-s epochs were saved and averaged. Power analysis was carried out across delta (1–3 Hz), theta (>3–8 Hz), alpha (>8–12 Hz), and beta (>12–30 Hz) bandwidths for each electrode. This was done using fast Fourier transformation (FFT) phase (time) option with a Hanning taper. This approach averages raw waveforms initially (time domain averaging) and subsequently computes FFT, which thereby takes phase relationships into account. Overall, 88% of epochs were retained for analysis for both eyes closed and open data sets. Electrodes were grouped and averaged for the left TPJ (lTPJ; CP5, P3, P7), rTPJ (CP6, P4, P8), central (C3, CZ, C4), and frontal (F3, FZ, F4) regions for further analysis.

Regarding coherence analysis, back-to-back 3-s epochs were saved and averaged from each 2-min resting state data file. Complex demodulation was used in place of FFT in Curry for this purpose (Compumedics 2011). A minimum of 10% acceptable epochs were required to be

processed further. Minimum and maximum lag criteria for coherence values obtained were set at 2 and 10 ms, respectively. Electrodes were grouped into the same clusters as above, frontal (F3, FZ, F4), central (C3, CZ, C4), lTPJ (CP5, P7, P3), and rTPJ (CP6, P4, P8), for averaging of individual electrode pairings and further analysis as per below.

Data Analysis

All final statistical analyses were carried out in SPSS v. 22, IBM. Data were screened for normality and outliers. The latter were winsorized, and the appropriate procedures were adopted to manage the former (if distributions were nonnormal, transformations were conducted to reduce skew/kurtosis according to Tabachnick and Fidell (2013)). Post hoc tests with Bonferroni adjustments were used where appropriate. In contexts such as the present where multiple comparisons are conducted, control of family-wise error is a concern. Bootstrapping, a resampling method increasingly used in such contexts, selects and examines subsamples of a test population over numerous iterations (generally ≥1,000 subsamples are preferred) to provide more information and make inferences regarding overall sample parameters. Bootstrapping provides more robust, accurate, and conservative estimates of *P* values and confidence intervals. It also assists with the reduction of type I error risk, without compromising power (and therefore increasing type II error) (Romano et al. 2010; Westfall and Troendle 2008; Wright et al. 2011). Reviews of bootstrapping and its many applications are also available (Davison and Hinkley 1997; Efron and Tibshirani 1994). Bootstrapping was utilized in the case of significant findings to ensure these were robust (1,000 samples, bias corrected accelerated). Details on bootstrapping and procedures in SPSS v. 22 are available as Supplemental Materials at https://figshare.com/articles/Bootstrapping_in_SPSS_v_22/9275909.

Also available on figshare are Supplemental Tables/Figures (https://figshare.com/articles/Materials_supplementing_manuscript/8202107) and SPSS data files for resting state eyes closed (https://figshare.com/articles/rsEEG_eyes_closed_SPSS_file_JoN/8202137) and eyes open conditions (https://figshare.com/articles/rsEEG_eyes_open_SPSS_file_JoN/8202134), as well as for coherence analysis (https://figshare.com/articles/Coherence_data_SPSS_file/8202116).

RESULTS

Poststimulation Questionnaire

Participants appeared to be well blinded to sham (only 39% correctly guessing), whereas 63% correctly identified an active condition. However, a χ^2-test comparing correct responses versus incorrect/unsure responses was not significant ($P = 0.07$). All participants successfully completed stimulation. Two participants temporarily ceased due to discomfort but completed stimulation after a short break (1–3 min). A graphical summary of stimulation blinding and a table detailing stimulation-related experience/sensations is available on figshare at https://figshare.com/articles/Post-stimulation_questionnaire_results/8869208.

Resting State Power Analysis

Eyes closed. Separate ANOVAs were used for frontal, central, and temporoparietal clusters, with log transformed power (uV^2) data. To examine possible hemispheric effects regarding the left and right TPJ clusters, a mixed model ANOVA with factors of time (pre and post), hemisphere (lTPJ and rTPJ), and condition (sham, cathodal, and anodal) examined the impacts of stimulation on spectral power at each bandwidth. Results were nonsignificant for lower frequencies (delta, theta, and alpha; see Supplemental Table S1). A significant time × hemisphere × condition interaction was found at the beta bandwidth [$F(2,50) = 3.69$, $P = 0.032$, $\eta_p^2 = 0.13$; Supplemental Table S2 and Supplemental Fig. S1). Post hoc analyses, however, were not significant. Mixed model ANOVAs (with factors of time and condition only) were also conducted separately for frontal and central clusters. Results were not significant (Supplemental Tables S3 and S4).

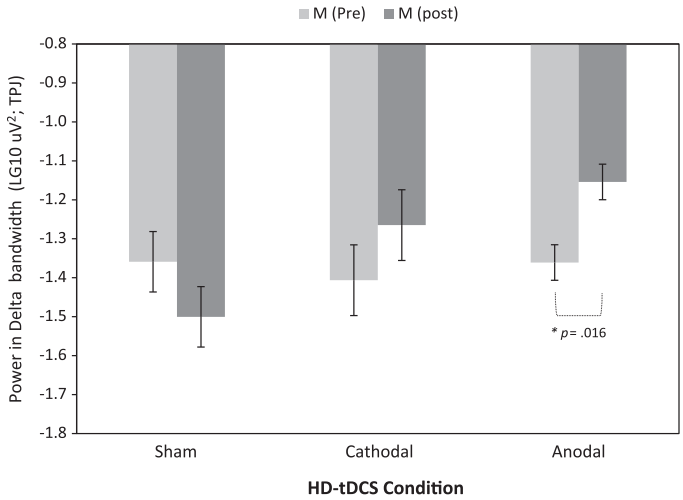

Fig. 3. Effect of condition (sham, cathodal, and anodal) on temporoparietal junction (TPJ) delta power [pooled across right (r)TPJ and left (l)TPJ, log transformed uV^2] during resting state (eyes open). HD-tDCS, transcranial direct current stimulation. Note: error bars represent SE; $P = 0.019$ after bootstrapping in anodal condition.

Eyes open. The same analyses were conducted for eyes open resting state data (also log transformed). Results were not significant for higher frequencies (Supplemental Tables S5–7). There was no significant time × hemisphere × condition interaction for rTPJ versus lTPJ at any bandwidth. However, time × condition interactions were found in the delta bandwidth for the TPJ [$F(2,49) = 5.08$, $P = 0.010$, $\eta_p^2 = 0.17$) and central clusters [$F(2,49) = 3.51$, $P = 0.037$, $\eta_p^2 = 0.13$] and in the theta bandwidth for the frontal cluster [$F(2,49) = 4.27$, $P = 0.019$, $\eta_p^2 = 0.15$]. A trend time × condition interaction was also found in the delta bandwidth for the frontal cluster [$F(2,49) = 3.19$, $P = 0.050$, $\eta_p^2 = 0.12$]. Post hoc analyses suggested that delta power was increased after anodal stimulation in both the TPJ [$t(15) = -2.71$, $P = 0.016$, $\eta^2 = 0.33$, Fig. 3; $P = 0.019$ after bootstrapping] and central clusters [$t(15) = -2.22$, $P = 0.042$, $\eta^2 = 0.25$, Fig. 4; $P = 0.052$ after bootstrapping], although the latter does not withstand Bonferroni correction at the revised alpha level of 0.0167 (and inflates to $P > 0.05$ with bootstrapping) and can be considered trend only (see also box and whisker representations of Fig. 3 and Fig. 4 at https://figshare.com/articles/Figure_3_1_Box_and_whiskers_plot_of_TPJ_delta_power_rsEO_/8947439 and https://figshare.com/articles/Figure_4_1_Box_and_whiskers_plot_of_central_delta_power_rsEO_/8947445, respectively. The former must be interpreted with caution also given that the *P* value is marginally >0.0167 also after bootstrapping. In frontal regions, power was increased after cathodal stimulation in both the theta bandwidth [$t(17) = -3.44$, $P = 0.003$, $\eta^2 = 0.44$, Fig. 5; $P = 0.002$ after bootstrapping] and delta bandwidth [$t(17) = -3.04$, $P = 0.007$, $\eta^2 = 0.38$, Fig. 6; $P = 0.003$ after bootstrapping]. Please note that these figures display log trans-

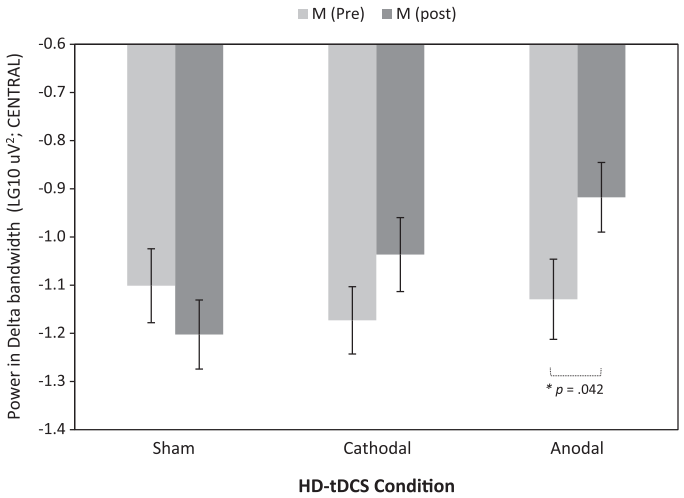

Fig. 4. Effect of condition (sham, cathodal, and anodal) on delta power (pooled across central electrodes, log transformed uV^2) during resting state (eyes open). HD-tDCS, transcranial direct current stimulation. Note: error bars represent SE; $P = 0.052$ after bootstrapping in anodal condition.

formed means (see also box and whiskers representations at https://figshare.com/articles/Figure_5_1_Box_and_whiskers_plot_of_frontal_theta_power_rsEO_/8947448 and https://figshare.com/articles/Figure_6_1_Box_and_whiskers_plot_of_frontal_delta_power_rsEO_/8947454, respectively). Several main effects of time were also observed (Supplemental Tables S5–S10).

Coherence Analysis

Coherence value difference scores (prestimulation subtracted from poststimulation) were used due to improved distribution normality compared with pre- and postdistributions, meaning that data transformations were not necessary for coherence analyses. Difference scores were calculated for each preidentified electrode pairing for each participant at each bandwidth, averaged across epochs (e.g., F3–CP6, F3–P4, F3–P8). These were then averaged across each region cluster pairing: rTPJ-frontal (CP6, P4, P8–F3, FZ, F4), rTPJ-central

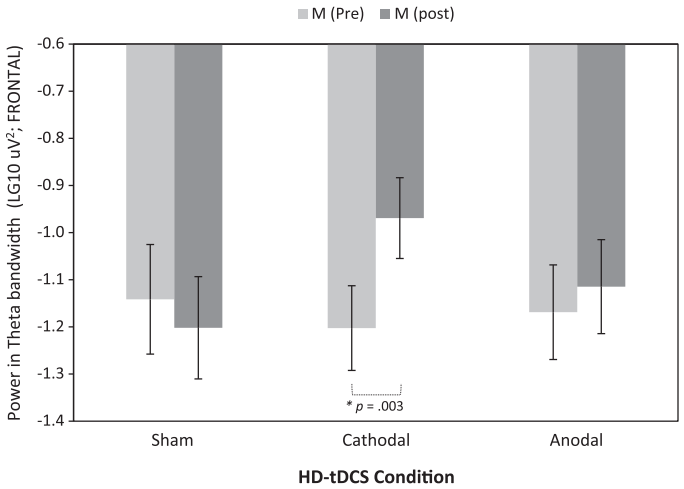

Fig. 5. Effect of condition (sham, cathodal, and anodal) on theta power (pooled across frontal electrodes, log transformed uV^2) during resting state (eyes open). HD-tDCS, transcranial direct current stimulation. Note: error bars represent SE; $P = 0.002$ after bootstrapping in cathodal condition.

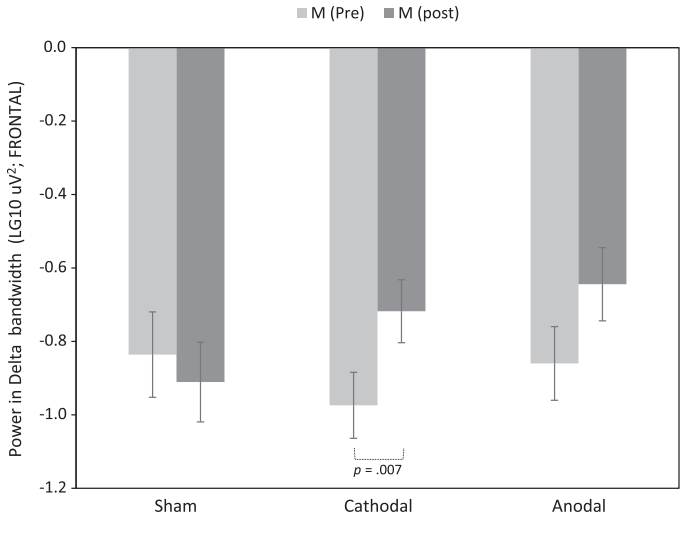

Fig. 6. Effect of condition (sham, cathodal, and anodal) on delta power (pooled across frontal electrodes, log transformed uV^2) during resting state (eyes open). HD-tDCS, transcranial direct current stimulation. Note: Error bars represent SE; $P = 0.003$ after bootstrapping in cathodal condition.

(CP6, P4, P8–C3, CZ, C4), and rTPJ-lTPJ (CP6, P4, P8–CP5, P7, P3). Only coherence pairs that begin and terminate in different regions were used for the averaged data.

Eyes closed. An average of 87% of cases were retained for analyses (Supplemental Table S11). One-way ANOVAs examined coherence difference scores (post-pre) in each cluster pairing at each bandwidth, with stimulation condition as the factor. Results were nonsignificant in all cases (Supplemental Table S12).

Eyes open. The same analyses were conducted for eyes open data. An average of 93% of cases were retained for analyses (Supplemental Table S13). Although rTPJ-central region pairings neared significance in the theta band (see Supplemental Table S14 for full summary statistics), the only statistically significant difference observed was in the rTPJ-lTPJ pairing in the delta band [$F(2,49) = 3.90$, $P = 0.027$, $\eta_p^2 = 0.14$]. Post hoc analyses suggested that rTPJ-lTPJ delta power coherence was increased after anodal stimulation compared with cathodal stimulation [$t(32) = 2.70$, $P = 0.011$ ($P = 0.012$ after bootstrapping), $\eta^2 = 0.19$] and sham stimulation [$t(32) = 2.10$, $P = 0.043$ ($P = 0.041$ after bootstrapping), $\eta^2 = 0.12$], although the latter does not withstand Bonferroni correction at the revised alpha level of 0.0167 and can be considered trend only. Figure 7 displays this result graphically (see also box and whiskers representation at https://figshare.com/articles/Figure_7_1_Box_and_whiskers_plot_of_rTPJ-lTPJ_delta_coherence_rsEO_/8947457. Positive mean differences indicate increased coherence between regions after stimulation and therefore increased rTPJ-lTPJ coherence after anodal stimulation in the delta bandwidth (compared with cathodal, and trending compared with sham).

DISCUSSION

This study applied anodal, cathodal, or sham HD-tDCS to the rTPJ to examine local and distributed modulatory effects at a neurophysiological level, via resting state EEG power and coherence. To our knowledge it is the first study to do so. The

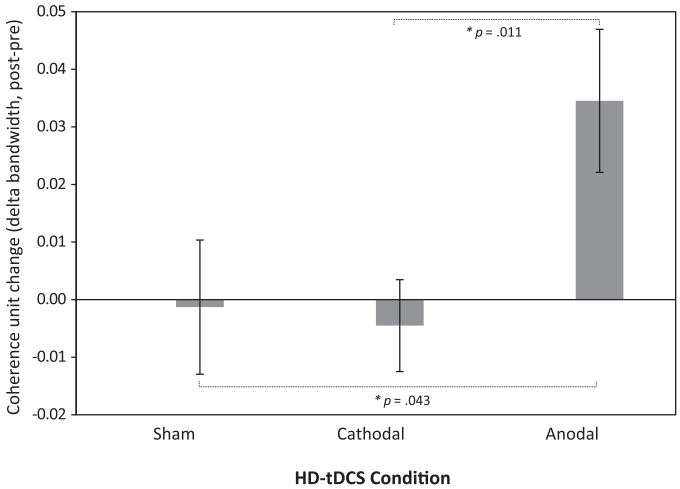

Fig. 7. Effect of condition (sham, cathodal, and anodal) on right and left temporoparietal junction (rTPJ-lTPJ) coherence (post-pre stimulation difference) in delta bandwidth during resting state (eyes open). HD-tDCS, transcranial direct current stimulation. Note: error bars represent SE; $P = 0.012$ after bootstrapping for anodal-cathodal comparison; $P = 041$ after bootstrapping for anodal-sham comparison.

results of the present study can be both compared and contrasted with prior findings that informed the present hypotheses (which were only partially supported) and will be discussed according to the following themes: *1*) active HD-tDCS modulated both local and network resting state power, but this occurred at low frequencies (particularly in the delta bandwidth) and not in the alpha/beta bandwidths as previously reported; *2*) anodal HD-tDCS increased lTPJ-rTPJ interhemispheric coherence in the delta bandwidth only; *3*) modulatory effects were almost exclusively observed in the eyes open (EO) rather than eyes closed (EC) condition, directly contrasting with prior groups findings.

Delta/Theta Power Modulated by Active HD-tDCS

In contrast to prior findings (Mangia et al. 2014; Spitoni et al. 2013), active stimulation did not increase resting state power in alpha or beta bandwidths. This null finding, however, is consistent with Hsu et al. (2014), who used the same tDCS protocol (targeting P4) as the other groups in attempting to increase alpha power but found no alpha modulation after anodal stimulation in what were categorized as high performers on a subsequent visual memory task and reduced alpha power in low performers. The authors interpreted this as a priori state/trait-based network oscillatory differences leading to differences in susceptibility/modulability by tDCS. Such individual differences may have contributed to variation in the present sample that reduced the power to detect higher frequency modulatory effects. Another difference between the present and prior studies is the use of HD-tDCS, which uses much smaller electrodes with greater current densities to elicit more localized stimulation effects. Such differences may also lead to different local and network neural/neurotransmitter impacts that result in different oscillatory profile effects.

The consistent finding of increases in delta power across frontal regions after cathodal stimulation and central/temporoparietal regions after anodal stimulation (in some instances trend only) was interesting and somewhat unexpected. That cathodal stimulation specifically modulated distal frontal regions in contrast to the more proximal regions modulated by anodal stimulation raises questions regarding differing oscillatory influences and mechanisms of action of the two current polarities, although the present methodology cannot shed further light on this potential distinction. More broadly, delta-power increases after cathodal motor cortex tDCS have been previously observed (Ardolino et al. 2005) and are consistent with the anodal-excitation/cathodal-inhibition (Ae/Ci) hypothesis of tDCS neuronal excitability effects: if cathodal stimulation inhibits, increased slow-wave power might be expected. Increased delta power after anodal stimulation contrasts with many prior studies (Annarumma et al. 2018; Keeser et al. 2011; Wirth et al. 2011), though these involve frontal rather than temporoparietal stimulation. Consistent with current findings, however, Boonstra et al. (2016) observed anodal stimulation increases in resting state delta power after frontal tDCS. These authors highlighted the relevance of EO versus EC resting state conditions, a point that will be pursued further below. They also interpreted this deviation from prior findings from the perspective of differing electrode size and current densities, noting that increased charge densities and therefore stimulation intensities can alter and even reverse normal Ae/Ci effects in the motor cortex. In one such study, 20 min of 2-mA cathodal tDCS (as applied here) produced increased cortical excitability rather than inhibition (Batsikadze et al. 2013). In general, the present study also adds support to the notion that the traditional Ae/Ci model of tDCS effects is problematic, particularly in nonmotor regions, and may also be state dependent and influenced by intra- and interindividual differences not controlled or accounted for in studies such as the present one (Horvath et al. 2014; Krause and Cohen Kadosh 2014).

The finding that delta/theta power in frontal regions increased after cathodal stimulation is, however, consistent with the traditional Ae/Ci perspective. While this has been observed previously at a local level in the motor cortex (Ardolino et al. 2005), this was not reported after rPPC cathodal stimulation in another study (Spitoni et al. 2013). Mangia et al. (2014), however, did find an increase in theta power during anodal rPPC stimulation that began locally and propagated forward to frontocentral regions after stimulation and particularly frontal regions in the EO condition. As above, methodological differences between studies, such as varying charge densities, may at least partly explain the inconsistent findings. The potential meaning and implication of these findings will be discussed after some brief statements on the coherence findings, as these are also relevant to the interpretation.

Anodal HD-tDCS Increased lTPJ-rTPJ Coherence in the Delta Bandwidth Only

Consistent with the themes above, interhemispheric TPJ delta coherence was increased after anodal stimulation. Combined with the increases in distributed resting state delta power poststimulation noted above, these findings raise questions regarding both the importance of slow wave activity to distal communication/connectivity, and the potential functional implications of such modulations, given the proposed roles of the rTPJ. While slow-frequency resting state oscillations have traditionally been associated with drowsy and sleep states (Annarumma et al. 2018), it is unlikely that the present results can be interpreted through a lens of increased drowsiness as the

study session progressed. If this were the case, increased slow wave power and coherence might be expected after sham compared with active stimulation, and in the EC rather than EO condition, the reverse of the pattern observed here.

Informing alternative interpretations, it is increasingly recognized that delta-oscillatory activity may have other functional significance in both the resting and task-oriented brain (Harmony 2013). In a detailed review, Knyazev (2012) posits a critical role for delta oscillations in terms of synchronizing cortical and autonomic functions, listing motivation/reward and attention/salience processes as strongly implicated. In another informative review, Harmony (2013) proposes a model that bridges the task-oriented/resting brain and sleep literature, by suggesting that delta oscillations may downmodulate the activity of brain networks not supporting current processing/mentation (for example, to inhibit sensory afferences and facilitate internally directed attention/concentration). This aligns with the GBI framework discussed in the INTRODUCTION (Jensen and Mazaheri 2010). Combined with the principle that large networks tend to be recruited during slow-wave oscillations (as opposed to higher frequencies association with more local networks) (Lu et al. 2007; Silberstein 2006; von Stein and Sarnthein 2000), it is plausible to hypothesize in the context of present results that slow wave oscillatory activity might be one means by which the rTPJ might contribute to its proposed integrative effects and functions across domains and networks, including a role in mediating between endogenous/exogenous attention and processing and influencing the activity of relevant and irrelevant networks. Frontoparietal and interhemispheric lTPJ-rTPJ structural and functional connectivity may be particularly important in this regard.

Modulatory Effects Were Almost Exclusively Observed in the EO Rather Than EC Condition

Prior papers, including two rPPC tDCS studies (Mangia et al. 2014; Spitoni et al. 2013), tend to find greater oscillatory responsiveness to tDCS in the EC rather than EO condition. More general research into differences between EO and EC conditions in EEG suggests a general reduction in delta, theta, and alpha power in EO compared with EC, taken to reflect the processing of visual stimuli necessitating higher frequency oscillations in relevant networks (Barry et al. 2007, 2009). More specifically, Mangia et al. (2014, p. 6) apply this to their interpretation by suggesting that the brain may have a greater sensitivity to tDCS in the EC condition as "a consequence of a higher processing capability to the external tDCS stimuli available."

While it is possible our differing result is the consequence of methodological differences or statistical anomaly, alternative interpretations are available in line with the rTPJ functional connectivity discussed in *Anodal HD-tDCS Increased lTPJ-rTPJ Coherence in the Delta Bandwidth Only*. More specifically, it is well established that the brain is not "resting" during so called resting states, despite the absence of exogenous visual input in EC conditions. Of relevance here is the proposed default mode network (DMN), a network of structures including the bilateral TPJ and medial frontal regions that tend to be more active "at rest" (or during endogenous attention processes such as autobiographical memory retrieval, considering the perspectives of others, and imagining future situations) and anticorrelated with exogenous or task-focused attention networks (Buckner et al. 2008; Greicius et al. 2003; Mars et al. 2012a). It is unlikely that in EO conditions, such as the current one, where participants are asked to gaze at a fixation cross on a screen for several minutes, that they can or do consciously attend to the cross for that duration. It is more likely that after a brief period participants continue to gaze at the cross as their mind "wanders" in the manner described above, implicating DMN activity and associated anticorrelated deactivations.

Consistent with this, Yan et al. (2009) examined functional connectivity and regional amplitude of low-frequency fluctuation (ALFF) in DMN regions in three resting state functional MRI conditions: EC, EO (with fixation; EO-F), EO (without fixation; EO-WF). They reported greater functional connectivity and ALFF in DMN regions in both EO conditions compared with EC, and greater functional connectivity in many regions (as well as ALFF in some regions) in EO-F compared with EO-WF. Yan et al. (2009, p. 9) take this to reflect more highly synchronized and greater spontaneous neuronal activity in DMN regions in EO compared with EC conditions and suggest that EO conditions may be associated with "more nonspecific or nongoal-directed visual information gathering and evaluating, as well as mind wandering and daydreaming." While speculative, linking this with the present discussion and results, one interpretation might be that in EO conditions increased DMN activity associated with activities such as episodic memory processing or mind wandering might require more downregulation of sensory afferences (and their salience attributions), particularly exogenous visual stimuli processing, and that broad low-frequency oscillatory network activity may be one means by which this is achieved. Furthermore, if this is more "effortful" in active conditions, this might partly explain why active rTPJ stimulation conditions exerted low-frequency network oscillatory activity influences in EO conditions only. Contrasting again with a prior rPPC tDCS study, Spitoni et al. (2013) verbally requested participants open or close eyes every 30 s for 15 min, which would have different network dynamic effects to the protocol used here (2 min of EO, 2 min of EC) and would mean the initial network effects/response to opening one's eyes (i.e., the effects of the visual input and the period of the system inhibiting these afferences if wishing to return to DMN processing) would make up a greater percentage of epochs used for resting state analysis and likely produce very different results.

Limitations

One important methodological limitation is the partial EEG montage. While this was partly necessary given the physical interference of HD-tDCS electrodes, it does limit both spatial resolution and the capacity to assess more global effects. Adding to this, electrode potentials were grouped and averaged for a priori regions of interest for final analyses, further reducing spatial resolution. The use of mastoids as reference is also potentially a limitation in terms of EEG signal bias (Joyce and Rossion 2005). However, this was partially offset by averaging the mastoids for analysis. A further limitation was the sex imbalance in the cathodal condition, which had a higher male-to-female ratio than the anodal condition. While sex may interact with resting state EEG measures, a recent review suggests that evidence for this is minimal and inconsistent in

healthy samples and that such analyses in prior studies were secondary in nature and had not systematically examined resting state sex differences (Sanders 2017). An associated study directly testing resting state EEG sex differences found increased beta power (at three frontocentral electrode sites) as the only significant difference between sexes in in women compared with men (across a healthy group and a group with schizophrenia) (Sanders 2017). Similarly, state-dependent influences of tDCS may include factors relevant to sex such as hormone levels (Krause and Cohen Kadosh 2014). However, at present we are unaware of any evidence suggesting sex differences in resting state EEG outcomes related to tDCS effects in healthy samples, although the reverse, the absence of sex differences, has been reported (Accornero et al. 2014). It is therefore unlikely that sex would exert a significant influence in the present healthy and high-functioning (largely university sourced) sample, although the results should be interpreted cautiously in this regard. An additional limitation is the lack of behavioral outcome measures linked to proposed rTPJ functions, which reduces the capacity for the findings and present discussion to link strongly and directly with TPJ function. Finally, it must also be acknowledged that the study was likely underpowered, which may at least partially account for several of the null findings that counter present hypotheses or past results. Related to this is the possibility of type I error in the context of multiple comparisons without full Bonferroni adjustment. However, it is encouraging that all significant findings occurred only in slow-wave, EO, active stimulation conditions, and that *P* values were robust to bootstrapping. Given the relative dearth of HD-tDCS-EEG oscillation reports in nonmotor areas, we consider it important to report all analyses conducted and consider our statistical approach an appropriate compromise between risk of type I and type II error. Nonetheless, our results must be considered preliminary, be interpreted cautiously, and await further replication.

Conclusion

This study applied HD-tDCS to the rTPJ to examine neuromodulatory effects via resting state EEG power and coherence. The results suggested that modulations of oscillatory activity at low-frequency bandwidths (particularly delta) were more likely to occur than at higher frequencies and in EO compared with EC conditions. The results were not uniformly consistent with the traditional Ae/Ci model of tDCS effects, adding support to the notion that this model applies less reliably to nonmotor sites or may become more complex in terms of dependence on state/trait/topography differences in nonmotor regions. Although the present data set can only be considered preliminary, it does point to the need for further analysis of delta-oscillatory activity with respect to rTPJ function and connectivity. Future studies would benefit from larger sample sizes to examine subtle neuromodulatory effects and could also consider study designs that might inform a broader discussion. This might include the utilization of behavioral outcomes relevant to the different implicit rTPJ functional networks, and additional methodologies such as magnetic resonance spectroscopy that might assist with assessing tDCS effects on underlying neurotransmitter concentrations, which may in turn map on to local and distributed network activity and behavioral outcomes.

ACKNOWLEDGMENTS

We thank Charlotte Davies and Natalia Albein-Urios, who contributed to data collection, and George Youssef, who provided statistical advice.

GRANTS

P. G. Enticott is supported by a Future Fellowship from the Australian Research Council (FT160100077).

DISCLOSURES

No conflicts of interest, financial or otherwise, are declared by the authors.

AUTHOR CONTRIBUTIONS

P.H.D. and P.G.E. conceived and designed research; P.H.D. and M.K. performed experiments; P.H.D. and J.S.Y. analyzed data; P.H.D., M.K., J.S.Y., S.B., and P.G.E. interpreted results of experiments; P.H.D. and J.S.Y. prepared figures; P.H.D. drafted manuscript; P.H.D., M.K., J.S.Y., S.B., and P.G.E. edited and revised manuscript; P.H.D., M.K., J.S.Y., S.B., and P.G.E. approved final version of manuscript.

REFERENCES

Accornero N, Capozza M, Pieroni L, Pro S, Davì L, Mecarelli O. EEG mean frequency changes in healthy subjects during prefrontal transcranial direct current stimulation. *J Neurophysiol* 112: 1367–1375, 2014. doi:10.1152/jn.00088.2014.

Annarumma L, D'Atri A, Alfonsi V, De Gennaro L. The efficacy of transcranial current stimulation techniques to modulate resting-state EEG, to affect vigilance and to promote sleepiness. *Brain Sci* 8: 137, 2018. doi:10.3390/brainsci8070137.

Ardolino G, Bossi B, Barbieri S, Priori A. Non-synaptic mechanisms underlie the after-effects of cathodal transcutaneous direct current stimulation of the human brain. *J Physiol* 568: 653–663, 2005. doi:10.1113/jphysiol.2005.088310.

Barry RJ, Clarke AR, Johnstone SJ, Brown CR. EEG differences in children between eyes-closed and eyes-open resting conditions. *Clin Neurophysiol* 120: 1806–1811, 2009. doi:10.1016/j.clinph.2009.08.006.

Barry RJ, Clarke AR, Johnstone SJ, Magee CA, Rushby JA. EEG differences between eyes-closed and eyes-open resting conditions. *Clin Neurophysiol* 118: 2765–2773, 2007. doi:10.1016/j.clinph.2007.07.028.

Batsikadze G, Moliadze V, Paulus W, Kuo MF, Nitsche MA. Partially non-linear stimulation intensity-dependent effects of direct current stimulation on motor cortex excitability in humans. *J Physiol* 591: 1987–2000, 2013. doi:10.1113/jphysiol.2012.249730.

Bonnefond M, Kastner S, Jensen O. Communication between brain areas based on nested oscillations. *eNeuro* 4: ENEURO.0153-0116.2017, 2017. doi:10.1523/eneuro.0153-16.2017.

Boonstra TW, Nikolin S, Meisener AC, Martin DM, Loo CK. Change in mean frequency of resting-state electroencephalography after transcranial direct current stimulation. *Front Hum Neurosci* 10: 270, 2016. doi:10.3389/fnhum.2016.00270.

Buckner RL, Andrews-Hanna JR, Schacter DL. The brain's default network: anatomy, function, and relevance to disease. *Ann N Y Acad Sci* 1124: 1–38, 2008. doi:10.1196/annals.1440.011.

Buzsáki G, Anastassiou CA, Koch C. The origin of extracellular fields and currents–EEG, ECoG, LFP and spikes. *Nat Rev Neurosci* 13: 407–420, 2012. doi:10.1038/nrn3241.

Bzdok D, Langner R, Schilbach L, Jakobs O, Roski C, Caspers S, Laird AR, Fox PT, Zilles K, Eickhoff SB. Characterization of the temporo-parietal junction by combining data-driven parcellation, complementary connectivity analyses, and functional decoding. *Neuroimage* 81: 381–392, 2013. doi:10.1016/j.neuroimage.2013.05.046.

Carter RM, Huettel SA. A nexus model of the temporal-parietal junction. *Trends Cogn Sci* 17: 328–336, 2013. doi:10.1016/j.tics.2013.05.007.

Compumedics. *CURRY Neuroimaging Suite Installation and Tutorials: Multi-Modal Neuroimaging for CURRY 7*. Charlotte, NC: Compumedics, 2011.

Davison AC, Hinkley DV. *Bootstrap Methods and Their Application*. Cambridge, UK: Cambridge University Press, 1997.

Donaldson PH, Kirkovski M, Rinehart NJ, Enticott PG. Autism-relevant traits interact with temporoparietal junction stimulation effects on social cognition: a high-definition transcranial direct current stimulation and elec-

troencephalography study. *Eur J Neurosci* 47: 669–681, 2018. doi:10.1111/ejn.13675.

Donaldson PH, Kirkovski M, Rinehart NJ, Enticott PG. A double-blind HD-tDCS/EEG study examining right temporoparietal junction involvement in facial emotion processing. *Soc Neurosci* 1–16, 2019. doi:10.1080/17470919.2019.1572648.

Donaldson PH, Rinehart NJ, Enticott PG. Noninvasive stimulation of the temporoparietal junction: a systematic review. *Neurosci Biobehav Rev* 55: 547–572, 2015. doi:10.1016/j.neubiorev.2015.05.017.

Eddy CM. The junction between self and other? Temporo-parietal dysfunction in neuropsychiatry. *Neuropsychologia* 89: 465–477, 2016. doi:10.1016/j.neuropsychologia.2016.07.030.

Efron B, Tibshirani RJ. *An Introduction to the Bootstrap*. Boca Raton, FL: CRC, 1994.

Florin E, Baillet S. The brain's resting-state activity is shaped by synchronized cross-frequency coupling of neural oscillations. *Neuroimage* 111: 26–35, 2015. doi:10.1016/j.neuroimage.2015.01.054.

Fries P. A mechanism for cognitive dynamics: neuronal communication through neuronal coherence. *Trends Cogn Sci* 9: 474–480, 2005. doi:10.1016/j.tics.2005.08.011.

Fries P. Rhythms for cognition: communication through coherence. *Neuron* 88: 220–235, 2015. doi:10.1016/j.neuron.2015.09.034.

Geng JJ, Vossel S. Re-evaluating the role of TPJ in attentional control: contextual updating? *Neurosci Biobehav Rev* 37: 2608–2620, 2013. doi:10.1016/j.neubiorev.2013.08.010.

Greicius MD, Krasnow B, Reiss AL, Menon V. Functional connectivity in the resting brain: a network analysis of the default mode hypothesis. *Proc Natl Acad Sci USA* 100: 253–258, 2003. doi:10.1073/pnas.0135058100.

Harmony T. The functional significance of delta oscillations in cognitive processing. *Front Integr Nuerosci* 7: 83, 2013. doi:10.3389/fnint.2013.00083.

Horvath JC, Carter O, Forte JD. Transcranial direct current stimulation: five important issues we aren't discussing (but probably should be). *Front Syst Neurosci* 8: 2, 2014. doi:10.3389/fnsys.2014.00002.

Hsu TY, Tseng P, Liang WK, Cheng SK, Juan CH. Transcranial direct current stimulation over right posterior parietal cortex changes prestimulus alpha oscillation in visual short-term memory task. *Neuroimage* 98: 306–313, 2014. doi:10.1016/j.neuroimage.2014.04.069.

Igelström KM, Webb TW, Graziano MS. Neural processes in the human temporoparietal cortex separated by localized independent component analysis. *J Neurosci* 35: 9432–9445, 2015. doi:10.1523/JNEUROSCI.0551-15.2015.

Igelström KM, Webb TW, Kelly YT, Graziano MS. Topographical organization of attentional, social, and memory processes in the human temporoparietal cortex. *eNeuro* 3: ENEURO.0060-16.2016, 2016. doi:10.1523/ENEURO.0060-16.2016.

Jensen O, Mazaheri A. Shaping functional architecture by oscillatory alpha activity: gating by inhibition. *Front Hum Neurosci* 4: 186, 2010. doi:10.3389/fnhum.2010.00186.

Joyce C, Rossion B. The face-sensitive N170 and VPP components manifest the same brain processes: the effect of reference electrode site. *Clin Neurophysiol* 116: 2613–2631, 2005. doi:10.1016/j.clinph.2005.07.005.

Keeser D, Padberg F, Reisinger E, Pogarell O, Kirsch V, Palm U, Karch S, Möller HJ, Nitsche MA, Mulert C. Prefrontal direct current stimulation modulates resting EEG and event-related potentials in healthy subjects: a standardized low resolution tomography (sLORETA) study. *Neuroimage* 55: 644–657, 2011. doi:10.1016/j.neuroimage.2010.12.004.

Knyazev GG. EEG delta oscillations as a correlate of basic homeostatic and motivational processes. *Neurosci Biobehav Rev* 36: 677–695, 2012. doi:10.1016/j.neubiorev.2011.10.002.

Krause B, Cohen Kadosh R. Not all brains are created equal: the relevance of individual differences in responsiveness to transcranial electrical stimulation. *Front Syst Neurosci* 8: 25, 2014. doi:10.3389/fnsys.2014.00025.

Krause B, Márquez-Ruiz J, Cohen Kadosh R. The effect of transcranial direct current stimulation: a role for cortical excitation/inhibition balance? *Front Hum Neurosci* 7: 602, 2013. doi:10.3389/fnhum.2013.00602.

Kubit B, Jack AI. Rethinking the role of the rTPJ in attention and social cognition in light of the opposing domains hypothesis: findings from an ALE-based meta-analysis and resting-state functional connectivity. *Front Hum Neurosci* 7: 323, 2013. doi:10.3389/fnhum.2013.00323.

Lecrubier Y, Sheehan DV, Weiller E, Amorim P, Bonora I, Harnett Sheehan K, Janavs J, Dunbar GC. The Mini International Neuropsychiatric Interview (MINI). A short diagnostic structured interview: reliability and validity according to the CIDI. *Eur Psychiatry* 12: 224–231, 1997. doi:10.1016/S0924-9338(97)83296-8.

Li LM, Uehara K, Hanakawa T. The contribution of interindividual factors to variability of response in transcranial direct current stimulation studies. *Front Cell Neurosci* 9: 181, 2015. doi:10.3389/fncel.2015.00181.

Lu H, Zuo Y, Gu H, Waltz JA, Zhan W, Scholl CA, Rea W, Yang Y, Stein EA. Synchronized delta oscillations correlate with the resting-state functional MRI signal. *Proc Natl Acad Sci USA* 104: 18265–18269, 2007. doi:10.1073/pnas.0705791104.

Mangia AL, Pirini M, Cappello A. Transcranial direct current stimulation and power spectral parameters: a tDCS/EEG co-registration study. *Front Hum Neurosci* 8: 601, 2014. doi:10.3389/fnhum.2014.00601.

Mars RB, Neubert FX, Noonan MP, Sallet J, Toni I, Rushworth MF. On the relationship between the "default mode network" and the "social brain". *Front Hum Neurosci* 6: 189, 2012a. doi:10.3389/fnhum.2012.00189.

Mars R, Sallet J, Schüffelgen U, Jbabdi S, Toni I, Rushworth MF. Connectivity-based subdivisions of the human right "temporoparietal junction area": evidence for different areas participating in different cortical networks. *Cereb Cortex* 22: 1894–1903, 2012b. doi:10.1093/cercor/bhr268.neuroConn.

Oldfield RC. The assessment and analysis of handedness: the Edinburgh inventory. *Neuropsychologia* 9: 97–113, 1971. doi:10.1016/0028-3932(71)90067-4.

Romano JP, Shaikh AM, Wolf M. Multiple testing. In: *The New Palgrave Dictionary of Economics*, edited by Palgrave Macmillan. London, UK: Palgrave Macmillan, 2010. doi:10.1057/978-1-349-95121-5.

Rossi S, Hallett M, Rossini PM, Pascual-Leone A; Safety of TMS Consensus Group. Safety, ethical considerations, and application guidelines for the use of transcranial magnetic stimulation in clinical practice and research. *Clin Neurophysiol* 120: 2008–2039, 2009. doi:10.1016/j.clinph.2009.08.016.

Sanders KM. *Demographic Differences in Resting State EEG in Healthy Controls and Patients with Schizophrenia*. Loma Linda, CA; Loma Linda University, 2017. https://scholarsrepository.llu.edu/etd/488.

Sellaro R, Nitsche MA, Colzato LS. The stimulated social brain: effects of transcranial direct current stimulation on social cognition. *Ann N Y Acad Sci* 1369: 218–239, 2016. doi:10.1111/nyas.13098.

Silberstein RB. Dynamic sculpting of brain functional connectivity and mental rotation aptitude. In: *Progress in Brain Research*, edited by Neuper C, Klimesch W. Amsterdam, The Netherlands: Elsevier, 2006, p. 63–76, vol. 159.

Spitoni GF, Cimmino RL, Bozzacchi C, Pizzamiglio L, Di Russo F. Modulation of spontaneous alpha brain rhythms using low-intensity transcranial direct-current stimulation. *Front Hum Neurosci* 7: 529, 2013. doi:10.3389/fnhum.2013.00529.

Stagg CJ, Bachtiar V, Amadi U, Gudberg CA, Ilie AS, Sampaio-Baptista C, O'Shea J, Woolrich M, Smith SM, Filippini N, Near J, Johansen-Berg H. Local GABA concentration is related to network-level resting functional connectivity. *eLife* 3: e01465, 2014. doi:10.7554/eLife.01465.

Tabachnick BG, Fidell LS. *Using Multivariate Statistics* (6th ed.). Boston, MA: Pearson Education, 2013.

von Stein A, Sarnthein J. Different frequencies for different scales of cortical integration: from local gamma to long range alpha/theta synchronization. *Int J Psychophysiol* 38: 301–313, 2000. doi:10.1016/S0167-8760(00)00172-0.

Westfall PH, Troendle JF. Multiple testing with minimal assumptions. *Biom J* 50: 745–755, 2008. doi:10.1002/bimj.200710456.

Wirth M, Rahman RA, Kuenecke J, Koenig T, Horn H, Sommer W, Dierks T. Effects of transcranial direct current stimulation (tDCS) on behaviour and electrophysiology of language production. *Neuropsychologia* 49: 3989–3998, 2011. doi:10.1016/j.neuropsychologia.2011.10.015.

Womelsdorf T, Schoffelen JM, Oostenveld R, Singer W, Desimone R, Engel AK, Fries P. Modulation of neuronal interactions through neuronal synchronization. *Science* 316: 1609–1612, 2007. doi:10.1126/science.1139597.

Wright DB, London K, Field AP. Using bootstrap estimation and the plug-in principle for clinical psychology data. *J Exp Psychopathol* 2: 252–270, 2011. doi:10.5127/jep.013611.

Yan C, Liu D, He Y, Zou Q, Zhu C, Zuo X, Long X, Zang Y. Spontaneous brain activity in the default mode network is sensitive to different resting-state conditions with limited cognitive load. *PLoS One* 4: e5743, 2009. doi:10.1371/journal.pone.0005743.